Yukiko Tomooka*, Georg Rauter, Nicolas Gerig, Ryo Takeda, Philippe Cattin, and Manuela Eugster

Bending stiffness variability between a deployable robotic laser osteotome and its insertion device

https://doi.org/10.1515/cdbme-2022-0035

Abstract: Varying device stiffness on purpose can provide safety and performance improvements in interventions involving flexible minimal-invasive surgical robotic devices. For example, when flexible robotic devices are used for inserting minimal-invasive tools along curved paths into the knee joint for arthroscopy, a high device stiffness can allow precise path following where desirable. In contrast, when the minimal-invasive flexible device has reached its desired location inside the patient's body, decoupling the surgical tool (end-effector) from the flexible robotic insertion device can be beneficial in avoiding transferring disturbances such as vibrations to the robot-patient interaction. In this paper, we investigate bending stiffness variability in dependence on the length of a flexible supply channel. Our experiments have shown that bending stiffness in fact decreases with the length of the supply channel but the highest stiffness connection is not sufficiently rigid and we plan to implement a more rigid connection to allow precise path following during insertion.

Keywords: Robotic surgery, supply channel, variable stiffness, parallel robot, robotic endoscope, minimally invasive surgery, laser osteotomy.

1 Introduction

Up to today, the standard for cutting bone in surgical procedures was mechanical devices, such as milling cutters, drills, and saws. Laser osteotomy would have several advantages over these mechanical tools for cutting bone, such as faster bone healing, functional cuts, and improved depth control [1]. However, lasers depend on robotic assistance when deep cuts are required. Such deep cuts were achieved by repeated accurate laser movement across the same location [2]. In 2021, the first laser osteotome called CARLO® (AOT, Basel, Switzerland) was successfully released. However, procedures involving CARLO® required exposing the bone in an open surgery because direct access, i.e., line of sight, was necessary for laser cutting.

We aim to reduce the invasiveness of laser bone-cutting by developing a robotic endoscope that guides the laser to the bone without direct access, i.e., in a minimal-invasive manner. Our first target applications are minimally invasive knee arthroplasty and cartilage replacement surgery. Our latest prototype [3] consisted of several subsystems, including a robotic endoscope for minimally invasive insertion with a miniature parallel robot for accurate laser guidance mounted at its tip. The miniature parallel robot could move the laser in 3 degrees of freedom and would attach to the bone surface to increase the stability of laser positioning. The robotic endoscope housed a supply channel connected to the miniature parallel robot. This supply channel held the laser fiber and flexible shafts required for the miniature parallel robot's actuation (Figure 1). These flexible shafts were constructed of steel wire, wound into coils, alternately twisted in the right or left direction.

We have implemented a mechanism that allowed coupling/decoupling of the parallel robot from the robotic endoscope to minimize the transmission of external disturbances to the parallel robot during laser guidance. The decoupling was not a complete mechanical decoupling, because the supply channel must remain connected to the parallel robot. Therefore, a flexible connection, i.e., the flexible supply channel, remained between the robotic endoscope and the parallel robot (Figure 2). This flexible connection, i.e., the flexible supply channel, could be modulated by adjusting the distance between the parallel robot and the distal end of the robotic endoscope (see d in Figure 1). This distance adjustment was actuated and controlled by the actuation unit. A strong coupling of the parallel robot to the endoscope was reached by minimizing the distance d between the parallel robot and the distal end of the robotic endoscope, while a weak coupling (i.e., decoupling) involved increasing the distance d. The purpose of

***Corresponding author: Yukiko Tomooka,** BIROMED-Lab, Department of Biomedical Engineering, University of Basel, Gewerbestrasse 14, 4123 Allschwil, Switzerland, e-mail: yukiko.tomooka@unibas.ch
Georg Rauter, Nicolas Gerig, Manuela Eugster, BIROMED-Lab, Department of Biomedical Engineering, University of Basel, Allschwil, Switzerland
Philippe Cattin, CIAN, Department of Biomedical Engineering, University of Basel, Allschwil, Switzerland
Ryo Takeda, Laboratory of Deformation Control, Division of Mechanical and Aerospace Engineering, Faculty of Engineering, Hokkaido University, Hokkaido, Japan

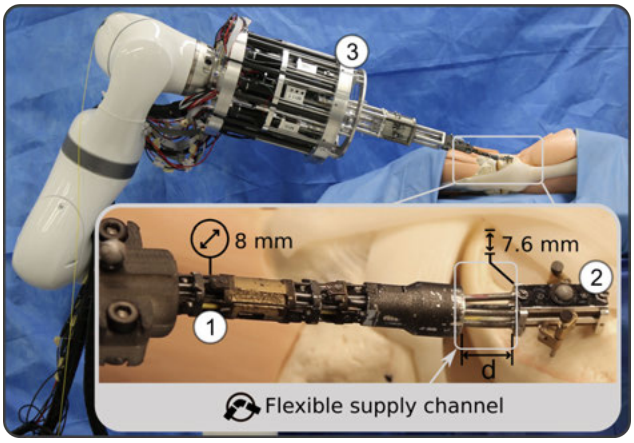

Fig. 1: Robotic system for minimally invasive laser osteotomy: Our latest prototype consisted of a robotic endoscope (1) with a miniature parallel robot (2) mounted at its tip. These components were controlled by the actuation unit (3), which was placed on a serial robot for large-scale manipulation in the operating room.

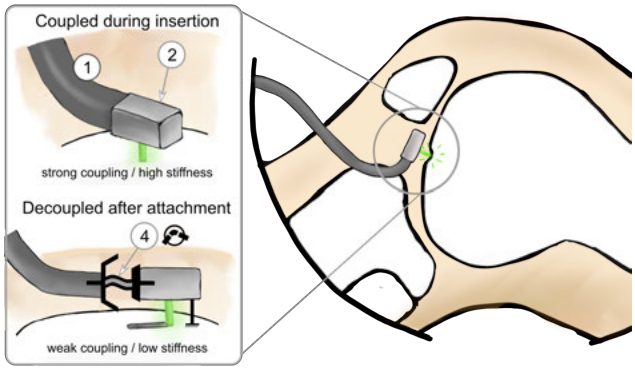

Fig. 2: During insertion, the miniature parallel robot (2) was rigidly coupled to the robotic endoscope (1). After attachment, the miniature parallel robot was decoupled, and a connection remained via the flexible supply channel (4).

a weak coupling was to minimize the transfer of disturbances and motions by proximal robot structures to the miniature parallel robot as soon as it was fixed close to the target tissue. In the contrary, also motions of the patient or the miniature robot during semi-autonomous laser osteotomy were not transferred back completely to the robotic endoscope. The strong coupling of the miniature parallel robot (end-effector) to the robotic endoscope was desired during device insertion and extraction to enable device guidance even along curved insertion paths in a teleoperated manner. Thus, the flexible, compliant connection could vary stiffness according to the current needs: precise end-effector insertion/extraction (high stiffness and strong coupling) along curved paths or semi-autonomous operation of the fixed end-effector during laser osteotomy with disturbance decoupling (low stiffness and weak coupling). Various strategies have been proposed to achieve variable stiffness for endoscopic instruments. Examples include linkage locking mechanisms [4] or granular jamming [5]. However, these strategies require additional components at the instrument tip to modify the stiffness, which make miniaturization more challenging. Therefore, we propose a concept without additional components for stiffness variation.

The supply channel consists of several parts (flexible shafts and optical fiber). Thus, it has a more complex structure than an elementary bending beam and is challenging to model accurately. To better understand and exploit the advantages of an elastic, flexible supply channel that allows varying the stiffness of the connection between the insertion structure (robotic endoscope) and the robotic end-effector (parallel robot) , we performed experiments to measure the bending stiffness of the flexible supply channel in dependence of channel length (distance d).

2 Methods

Because the supply channel was approximately rotationally symmetric, we measured one-dimensional bending stiffness in this first evaluation. We assumed that the mechanism only moves in one direction (z). With this assumption, we defined stiffness as

$$k = \frac{F_z}{\delta_z}, \tag{1}$$

with F_z being the force applied on the miniature parallel robot body in z-direction and δ_z the displacement of the body produced by this force.

The robotic endoscope (1) was oriented horizontally, and the miniature parallel robot (2) was placed above a force/torque sensor (5) (Nano17 with calibration SI-12-0.12, ATI Industrial Automation, USA), which was mounted on a manual translation stage (6) (PT1/M, Thorlabs Inc., USA) (Figure 3).

We performed measurements in four conditions ($d = 3\,\mathrm{mm}$, $d = 7\,\mathrm{mm}$, $d = 13\,\mathrm{mm}$, and $d = 17\,\mathrm{mm}$). The first minimum condition ($d = 3\,\mathrm{mm}$) represented the state in which the parallel robot is coupled to the robotic endoscope. The other three conditions represented decoupled states. For each condition, we performed three repetitions of the measurement (runs i, ii, and iii). Each measurement consisted of the following procedure: At first, the desired length of the supply channel (distance d) was set and verified by measurement with a Vernier caliper. Then, the force/torque sensor was zeroed. The force sensor was moved with the manual stage until the sensor detected contact with the miniature parallel robot. Subsequently, the force sensor was moved using the translation stage in four steps of $\delta_z = 2\,\mathrm{mm}$. After each step and a short initial settling time, we recorded an evaluation time of 10 seconds. The measurement data was collected via a

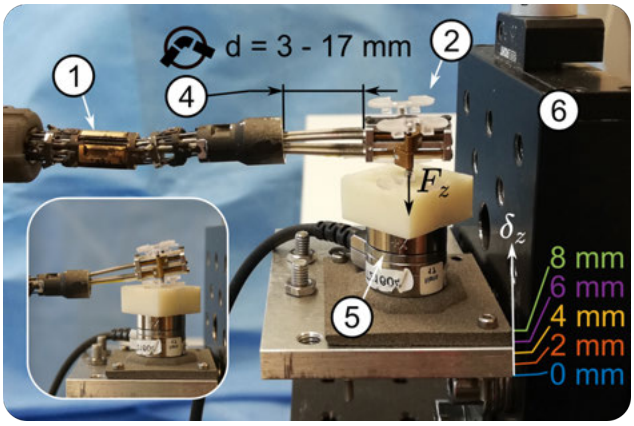

Fig. 3: Measurement setup to measure bending stiffness of the flexible supply channel (4) based on the force F_z and displacement δ_z. For description of the other labels refer to the manuscript text.

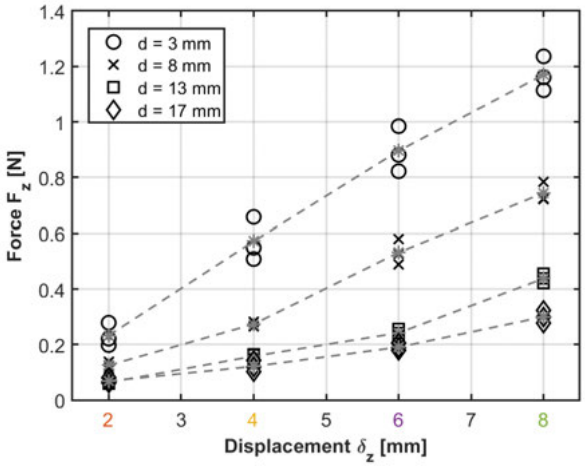

Fig. 4: Measured force F_z for different displacements δ_z. The different symbols refer to the different experiment conditions, i.e., distances d. The mean values over the three measurement runs are marked with a grey star and connected by a grey dashed line for each condition.

Speedgoat real-time target machine (Speedgoat, Switzerland) at a sample rate of 1 kHz.

The measurement data were analyzed using Matlab r2020b (Mathworks Inc., USA). The bending stiffness was calculated according to Equation 1. F_z was calculated as the mean value of the force in the $z-$direction of the force sensor coordinate system measured during the 10 seconds evaluation time and δ_z was the manually set linear stage displacement.

3 Results

The results showed that the bending stiffness of the flexible supply channel decreased as the channel length, i.e., the distance d, was increased (Figure 4). For more detailed values refer to Figure 5 and Table 1.

Tab. 1: Resulting bending stiffness k. The minimum and maximum values for each distance d are highlighted in bold.

Distance	Run	Stiffness k [N mm^{-1}]			
		δ_z = 2 mm	4 mm	6 mm	8 mm
d = 3 mm	i	0.139	**0.165**	0.164	0.155
	ii	0.111	0.137	0.147	0.145
	iii	**0.099**	0.127	0.137	0.139
d = 8 mm	i	0.069	0.068	0.097	**0.098**
	ii	**0.057**	0.067	0.081	0.090
	iii	0.062	0.070	0.088	0.091
d = 13 mm	i	**0.029**	0.036	0.038	0.053
	ii	0.033	0.041	0.043	**0.057**
	iii	0.033	0.041	0.040	0.055
d = 17 mm	i	0.040	0.036	0.034	**0.040**
	ii	0.033	0.030	0.031	0.037
	iii	0.030	**0.026**	0.030	0.035

4 Discussion

We measured bending stiffness of the flexible supply channel in dependence of four different channel lengths. The results showed the expected decrease in stiffness of the flexible supply channel as the channel length, i.e., the distance d, increased (Figure 4). This result indicates that the effect of the external disturbances on the positioning of the laser can be reduced by increasing the channel length (distance d), i.e., by introducing a weak coupling between the parallel robot and the robotic endoscope.

During insertion of the device into the patient, the parallel robot must be rigidly coupled to the endoscope to avoid a large deflection of the flexible supply channel and thus buckling of the parallel robot. According to a previous study, the lateral contact force during insertion of a rigid endoscope dummy into the knee of a body donor was in the range of $0-5$ N [6]. We measured that the parallel robot displaced 8 mm under the lateral force (F_z) of 1.2 N in the strongly coupled condition (d = 3mm) (Figure 4). This result indicates that a displacement (δ_z) larger than 8 mm can be expected during the insertion of the device into the knee.

Therefore, an additional mechanism to increase the coupling strength between the robotic endoscope and the parallel robot during device insertion will be required if a precise path following behavior is desired despite of inevitable interaction forces with the adjacent tissues. Possible concepts include granular jamming, which has also been proposed to vary the stiffness of joints [5], or inflatable balloons used in various surgical applications (e.g., balloon catheters for angioplasty).

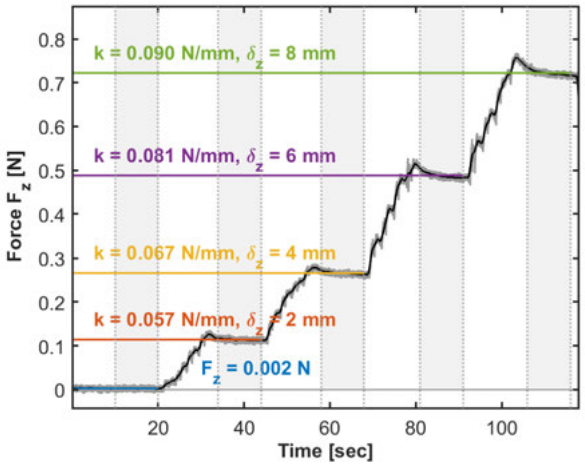

Fig. 5: The plot shows the measured force F_z (grey) and moving average (1000 samples) smoothed values (black). The manual performed deflections δ_z are color-coded. Only one (second) experiment run out of three is shown for only one condition ($d = 8\,\mathrm{mm}$). The values for the other runs and conditions can be found in Figure 4 and Table 1. The light grey vertical areas indicate the 10 seconds evaluation time. The colored lines indicate the calculated mean force values during the settling time labelled with corresponding stiffness value k.

We observed a deflection of the endoscope's most distal joint during the experiments when a large force was applied to the parallel robot. In the coupled state ($d = 3\,\mathrm{mm}$) the endoscope's most distal joint started to deflect at $\delta_z = 4\,\mathrm{mm}$. For the decoupled states, the endoscope's most distal joint started to deflect at $\delta_z = 8\,\mathrm{mm}$. Thus, the measured displacements in the coupled state also included a displacement of the robotic endoscope. Therefore, the actual bending stiffness of the flexible channel could be higher than measured. Thus, to avoid deflecting the device during insertion, it might also be required to stiffen the robotic endoscope's joints. Such additional stiffening could be achieved by implementing joint breaks or series elastic actuation [7]. To measure the supply channel's bending stiffness independently, the endoscope would have to be fixed during the measurement. In addition, the initial position of the parallel robot was set manually by observing the contact force values. Therefore, a distance between the force sensor and the parallel robot at the initial contact condition would have resulted in a lower measurement force. This could have caused the variation of the measured forces, i.e., the calculated stiffness (Table 1) between the runs. Although the measured bending stiffness k may include these influences, the reduction of the stiffness with increasing length of the flexible supply channel (distance d) shows the principle functionality of the decoupling concept.

5 Conclusion

We aim to minimize disturbances influencing the accuracy of the surgical instrument by decoupling the functional head of these surgical instruments (i.e., the parallel robot or other end-effectors) from the structures used for insertion (i.e., the robotic endoscope). We demonstrated that increasing the length of the flexible supply channel (distance d) decreased its bending stiffness. Therefore, it is feasible to reduce the propagation of forces. Further investigations considering damping effects are necessary to evaluate the reduction of external disturbances' transmission (e.g., vibration). In case higher stiffness of the system is desired such as during device insertion/extraction in a strongly coupled state, additional mechanisms to increase stiffness could be applied.

Acknowledgment: The authors gratefully acknowledge funding of the Werner Siemens Foundation through the MIRACLE project.

Author Statement

The authors have no conflict of interest to disclose.

References

[1] Augello M, Deibel W, Nuss K, Cattin P, Jürgens P. Comparative microstructural analysis of bone osteotomies after cutting by computer-assisted robot-guided laser osteotome and piezoelectric osteotome: an in vivo animal study. Lasers in Medical Science; 2018: 1471-1478.

[2] Burgner J. Robot-assisted laser osteotomy. Dissertation. Karlsruher Institute for Technology. 2010.

[3] Eugster M, Robotic system for accurate minimally invasive laser osteotomy. At - Automatisierungstechnik; 2022:70:676-678.

[4] Yagi A, Matsumiya K, Masamune K, Liao H, Dohi T. Rigid-flexible outer sheath model using slider linkage locking mechanism and air pressure for endoscopic surgery. Medical Image Computing and Computer-Assisted Intervention (MICCAI); 2006:503-510.

[5] Jiang A, Xynogalas G, Dasgupta P, Althoefer K, Nanayakkara T. Design of a variable stiffness flexible manipulator with composite granular jamming and membrane coupling. International Conference on Intelligent Robots and Systems (IROS); 2012.

[6] Eugster M, Zoller E, Fasel L, Cattin P, Friederich NF, Zam A, et al. Contact force estimation for minimally invasive robot-assisted laser osteotomy in the human knee. Joint Workshop on New Technologies for Computer/Robot Assisted Surgery (CRAS) 2018.

[7] Fasel L, Gerig N, Cattin P, Rauter G. Control evaluation of antagonistic series elastic actuation for a robotic endoscope joint. Journal of Bionic Engineering; 2022:1-10.